

Heat transport by lattice and spin excitations in the spin chain compounds SrCuO_2 and Sr_2CuO_3

A. V. Sologubenko, K. Giannò, H. R. Ott

Laboratorium für Festkörperphysik, ETH Hönggerberg, CH-8093 Zürich, Switzerland

A. Vietkine, A. Revcolevschi

Laboratoire de Physico-Chimie des Solides, Université Paris-Sud, 91405 Orsay, France

(September 14, 2021)

We present the results of measurements of the thermal conductivity of the quasi one-dimensional spin $S=1/2$ chain compound SrCuO_2 in the temperature range between 0.4 and 300 K along the directions parallel and perpendicular to the chains. An anomalously enhanced thermal conductivity is observed along the chains. The analysis of the present data and a comparison with analogous recent results for Sr_2CuO_3 and other similar materials demonstrates that this behavior is generic for cuprates with copper-oxygen chains and strong intrachain interactions. The observed anomalies are attributed to the one-dimensional energy transport by spin excitations (spinons), limited by the interaction between spin and lattice excitations. The energy transport along the spin chains has a non-diffusive character, in agreement with theoretical predictions for integrable models.

66.70.+f, 75.40.Gb, 63.20.Ls

I. INTRODUCTION

The physics of one-dimensional (1D) magnetic systems has been of interest for some time but particularly significant progress, both in experiment and theory, has been made during the last several years. The related research activities have been growing because the quantum nature of low-dimensional low-spin systems promises a rich variety of phenomena to be explored. Among other features, the transport of energy in 1D magnetic systems is expected to be highly unusual. A number of models describing one-dimensional systems are integrable, implying, for instance, conservation of energy current and, as a consequence, ballistic energy propagation and divergent thermal conductivity. The question whether the energy transport is diffusive or ballistic is currently under active discussion for atomic¹⁻³ as well as spin⁴⁻⁶ 1D systems.

The 1D Heisenberg $S=1/2$ systems with antiferromagnetic coupling between adjacent spins are of particular interest. It is well established that elementary excitations in such systems are not $S=1$ magnons but $S=1/2$ quantum solitons,⁷ commonly called spinons. Spinons can only be created or destroyed in pairs but they may be treated as free particles, at least at large spatial separation.^{8,9} The interaction of spinons, as quantum solitons, with structural defects and other quasiparticles, such as phonons, is poorly investigated both theoretically and experimentally, although in classical Heisenberg and Ising 1D magnetic systems, the interaction of solitons with defects, phonons, and magnons demonstrates a number of interesting features¹⁰⁻¹⁴ (for a review, see Ref. 15).

In order to probe the features of energy transport in $S=1/2$ Heisenberg chains, only a limited number of experiments, such as inelastic neutron scattering¹⁶ or NMR,¹⁷ is available. In case of a sufficiently strong cou-

pling between the phonon and the spin subsystems, the energy transport mediated by magnetic excitations can also be monitored via experiments probing the thermal conductivity. Although the spin-lattice interaction as well as the influence of defects and interchain interactions make the spin system non-integrable, an anomalous behavior of the spin-mediated thermal conductivity may, nevertheless, be expected. Establishing the heat transport carried by spin excitations may, in addition, reveal information concerning magnetic defects and the spin-lattice interaction. The spin-lattice interaction is very important in 1D magnetic system, because it leads to modifications of the spectrum of spin excitations¹⁸ and, under special circumstances, to the formation of new phases, such as the spin-Peierls dimerised state. Besides defects and phonons, interchain interactions are also anticipated to influence the energy transport in the spin system and hence may be probed by thermal-conductivity experiments.

In previous work concerning the thermal conductivity $\kappa(T)$ in quasi-1D $S=1/2$ Heisenberg systems, observations of some spin-mediated heat transport, in addition to the dominant phonon contribution, have been reported for KCuF_3 ,¹⁹ CuGeO_3 ,²⁰ and Yb_4As_3 .²¹ The most pronounced effects, however, have been observed in $(\text{Sr,Ca})_{14}\text{Cu}_{24}\text{O}_{41}$, containing double-leg Cu-O ladders with 180° Cu-O-Cu bond angles.^{22,23} The thermal conductivity along the ladder direction exhibits an anomalous double-peak temperature dependence. It has fairly well been established by a detailed analysis²² that this two-peak feature in $\kappa(T)$ of $(\text{La,Sr,Ca})_{14}\text{Cu}_{24}\text{O}_{41}$ is caused by two main contributions, one due to phonons, responsible for the low-temperature peak, and the other due to itinerant spin excitations in the ladders, causing the additional high-temperature maximum.

In order to test the above mentioned conjectures con-

cerning energy transport by spin excitations in $S=1/2$ 1D Heisenberg systems, we have investigated the low-temperature thermal conductivities of two materials containing 180° Cu-O chains, namely SrCuO_2 and Sr_2CuO_3 . The crystallographic unit cells^{24,25} of the two compounds are schematically drawn in Fig. 1. The intrachain exchange coupling J of 2100–3000 K^{26–29} in these two materials is of the same order of magnitude as the interactions along the ladder legs in $\text{Sr}_{14}\text{Cu}_{24}\text{O}_{41}$ ($J=1510$ K).³⁰ The compounds considered here exhibit different arrangements of the same type of chains. The structure of Sr_2CuO_3 contains Cu-O chains with a very small interchain interaction J' ($\alpha \equiv J'/J \sim 10^{-5}$).²⁸ SrCuO_2 is built by double Cu-O chains forming Cu-O ribbons containing Cu-Cu zig-zag chains (see Fig. 1). The interaction between the two chains occurs via 90° Cu-O-Cu bonds providing a weak ($|\alpha| = 0.1\text{--}0.2$) ferromagnetic interaction.³¹ For comparison, the chains forming the double-leg ladders in $(\text{Sr,Ca})_{14}\text{Cu}_{24}\text{O}_{41}$ are connected via 180° Cu-O-Cu bonds (“rungs”), therefore for the ladders $\alpha = 0.55$ is rather large.³⁰ The spin excitation spectrum for the single-chain compound Sr_2CuO_3 is gapless. Because the interaction between the chains forming the Cu-O ribbons in the SrCuO_2 is ferromagnetic, the excitation spectrum remains gapless,³² in contrast to the gapped spectrum of spin ladders where the interaction between the chains is antiferromagnetic.

In this paper, we present new experimental results on the thermal conductivity of SrCuO_2 along the main crystallographic directions in the temperature region between 0.4 and 300 K. These data are analyzed together with those for Sr_2CuO_3 measured and presented previously.³³ We offer a detailed analysis of phonon and spinon contributions to the thermal conductivity along different crystallographic directions. We show that the thermal transport perpendicular to the chain direction is predominantly phononic at all temperatures, whereas along the chain direction the spinon contribution is dominant at elevated temperatures. The scattering of phonons is mainly via other phonons, at dislocations, and at sample boundaries. The spinon thermal conductivity may reliably be evaluated only in the high temperature region above 60 K where it is predominantly limited by the spin-lattice interaction. At very low temperatures, the spin-lattice interaction appears to be rather weak and therefore the intrinsic spinon thermal conductivity cannot be observed.

For clarity we introduce an auxiliary notation of crystallographic directions. For both compounds we denote the direction along the chains as c' (c for SrCuO_2 and b for Sr_2CuO_3), the direction perpendicular to the CuO squares as b' (a for SrCuO_2 and c for Sr_2CuO_3), and the direction in the CuO square plane but perpendicular to the chains as a' (see Fig. 1). This notation is compatible with the crystallographic axes of the spin-ladder system $(\text{Sr,Ca})_{14}\text{Cu}_{24}\text{O}_{41}$, for which a' , b' , and c' correspond to the a , b , and c directions, respectively.

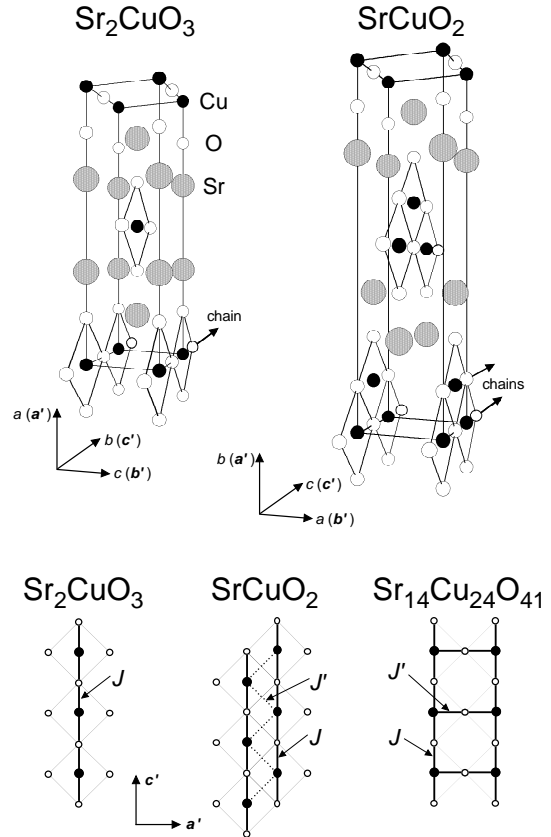


FIG. 1. The schematic unit cells of the crystal structures of SrCuO_2 and Sr_2CuO_3 . For each material, the layout of the Cu-O chains is emphasized. For comparison, the structure of the ladder in $\text{Sr}_{14}\text{Cu}_{24}\text{O}_{41}$ is also shown.

II. EXPERIMENTAL DETAILS

The single crystals of SrCuO_2 and Sr_2CuO_3 were grown by a traveling-solvent floating-zone method.³⁴ The high structural quality of the crystals was confirmed by neutron diffraction experiments.³⁴

From each crystal, three specimens in the form of rectangular bars with typical dimensions $2.5 \times 1 \times 1$ mm³ and with the longest dimension parallel to each principal axis were cut with a thin-blade diamond saw. The thermal conductivity was measured by a standard steady-state heat-flow technique, fixing the sample at one end to a heat sink. The temperature gradient along the sample was produced by a heater (1 k Ω chip resistor) glued to the opposite end of the sample, and monitored in overlapping temperature ranges by a matched pair of RuO_2 thermometers at $T < 5$ K and by differential Chromel-Au + 0.07% Fe thermocouples at higher temperatures. The temperature difference between the thermometers was typically 1.5% of the absolute mean temperature of the sample. The estimated accuracy of $\pm 10\%$ of the absolute value of $\kappa(T)$ is mainly caused by the uncertainty of the sample geometry, the relative error being of the

order of 0.5% of the measured values of κ .

III. EXPERIMENTAL RESULTS

The results of the thermal conductivity measurements for SrCuO_2 are presented in Fig. 2, together with our previous results³³ on the thermal conductivity of Sr_2CuO_3 . For both materials $\kappa(T)$ reveals similar general features. In particular, the thermal conductivities along the directions perpendicular to the chains ($\kappa_{a'}$, $\kappa_{b'}$) are similar not only in their features of the temperature dependence, but even in absolute values. At the same time, the thermal conductivity along the chains is distinctly higher than $\kappa(T)$ perpendicular to the chains in both cases. This is particularly evident at temperatures above the $\kappa(T)$ maxima. At room temperature, this excess conductivity for the double-chain material SrCuO_2 exceeds that for the single-chain compound Sr_2CuO_3 by almost a factor of two. In the temperature region between 1 and 6 K, where magnetic phase transitions have been reported for both materials,^{35–38} no anomalous features in $\kappa(T)$ have been observed. Since these transitions are indicated by anomalies of the magnetic specific heat,^{33,37} the interaction between the spin and the lattice systems as well as the spin contribution to the measured thermal conductivity must be negligible in this temperature region for both materials.

Because both SrCuO_2 and Sr_2CuO_3 are electrical insulators, electrons do not participate in the heat transport. Below, we thus analyze the experimental data assuming that the main heat carriers are phonons and spin excitations.

IV. ANALYSIS OF THE PHONON CONTRIBUTION

A. The model and fitting procedure

In general, the behavior of the phonon thermal conductivity $\kappa_{\text{ph}}(T)$ is determined by scattering of phonons by structural defects, phonons and other quasiparticles. At temperatures $T \geq \Theta_D$, where Θ_D is the Debye temperature, the phonon-phonon Umklapp-processes (U-processes) usually dominate and it often turns out that $\kappa_{\text{ph}} \propto T^{-\alpha}$, where $\alpha \sim 1$. The mean free path of the phonons is very small and comparable to interatomic distances. At temperatures below Θ_D the probability of U-processes decreases exponentially and the phonon mean free path increases accordingly. The maximum mean free path of phonons, normally reached only at very low temperatures, is limited by the size of a sample. At this, so called Casimir limit, the thermal conductivity may be calculated by $\kappa_{\text{ph}} = 1/3 C_{\text{ph}} v L_b$, where C_{ph} is the lattice specific heat, v is the average sound velocity along the chosen direction, and L_b is a constant related to the

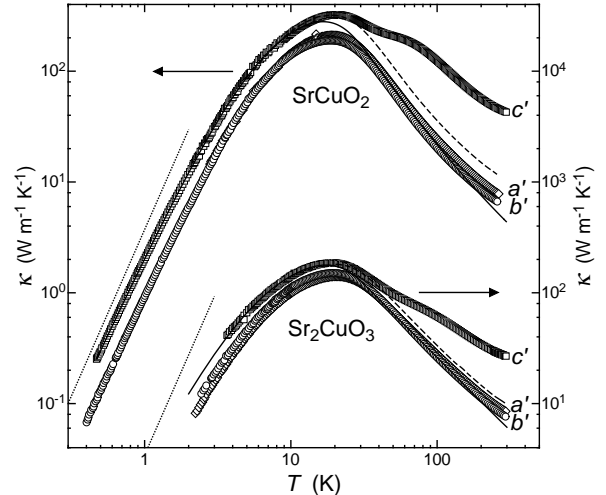


FIG. 2. Temperature dependences of the thermal conductivities of SrCuO_2 and Sr_2CuO_3 along the a' , b' , and c' axes. The dotted lines represent estimated limits of the thermal conductivity due to the finite size of the samples. The solid and dashed lines represent different evaluations of the phonon contribution to $\kappa_{c'}$ as described in the text.

sample size. Hence, for isotropic materials, $\kappa_{\text{ph}} \propto T^3$ at low temperatures. These two sources for scattering of phonons are always present in any material, generating some typical features of $\kappa_{\text{ph}}(T)$ including a distinct maximum at $T_{\text{max}} \leq \Theta_D/10$. Various defects, such as impurities, dislocations, stacking faults etc., also participate in phonon scattering, thereby reducing the thermal conductivity, especially in the region of T_{max} . Various quasiparticle excitations such as magnons, electrons, excitons etc. also influence the thermal conductivity by scattering phonons and by providing additional channels of heat transport.

In order to identify the dominant mechanisms of phonon scattering and to estimate their relative importance, we have fitted the experimental data by using the Debye approximation of the phonon spectrum combined with the relaxation-time approximation for calculating the thermal conductivity. The model assumes the same group velocities and relaxation rates for phonons of different polarizations. A more accurate and more complicated analysis, taking into account possible differences in the scattering rates for phonons of different polarisations, would require a detailed knowledge of elastic constants, which is still missing. The phonon thermal conductivity is thus calculated as

$$\kappa_{\text{ph}} = \frac{k_B}{2\pi^2 v} \left(\frac{k_B}{\hbar} \right)^3 T^3 \int_0^{\Theta_D/T} \frac{x^4 e^x}{(e^x - 1)^2} \tau(\omega, T) dx, \quad (1)$$

where ω is the frequency of a phonon, $\tau(\omega, T)$ is the corresponding relaxation time, Θ_D is the Debye temperature, and $x = \hbar\omega/k_B T$. As a further simplification we assume

that all mechanisms of phonon scattering act independently. In this case,

$$\tau^{-1} = \sum \tau_i^{-1}, \quad (2)$$

where each term τ_i^{-1} corresponds to an individual independent scattering mechanism. For instance,

$$\tau_b^{-1} = v/L_b \quad (3)$$

for phonon scattering by sample boundaries,

$$\tau_{pd}^{-1} = A\omega^4 \quad (4)$$

for phonon scattering by point defects (Rayleigh scattering), and

$$\tau_U^{-1} = B\omega^2 T \exp(-\Theta_D/bT) \quad (5)$$

for phonon-phonon U-processes. As indicated in Eq. (2), there may be other contributions to τ^{-1} , such as phonon-phonon N-processes, phonon-spin scattering, etc. In the first step only the three main mechanisms (boundaries, point defects and U-processes) were considered for all samples. In those cases where the fitting of the data with a reasonable accuracy failed, additional terms representing relevant scattering processes were introduced in Eq. (2).

For the fitting procedure we employed the Levenberg-Marquardt algorithm. The quantities L_b , A , B , and b , defined in Eqs. (3) to (5) were treated as freely adjustable parameters. The criterion of selecting additional terms in Eq. (2) was the minimization of the mean-square deviation χ^2 . We used the Θ_D values of 441 K for Sr_2CuO_3 (Ref. 33) and 357 K for SrCuO_2 (Ref. 39). The mean sound velocity v was calculated from the values of Θ_D , using the equation $v = \Theta_D (k_B/\hbar) (6\pi^2 n)^{-1/3}$, where n is the number density of atoms.

B. Phonon thermal conductivity perpendicular to the chain direction

As may be seen in Fig. 2, the thermal conductivities of SrCuO_2 and Sr_2CuO_3 in the directions perpendicular to the chains exhibit the temperature dependence that is typical for phonon heat transport. This includes $\kappa \propto T^{-1}$ at high temperatures and approaching $\kappa \propto T^3$ at low temperatures, the latter being expected if the phonon mean free path l_{ph} is constant. Since l_{ph} turns out to be shorter than the smallest sample dimensions even at 0.4K (for SrCuO_2), the influence of defects cannot be neglected.

It turns out that the three mechanisms initially included in Eq. (2) were not enough to fit the data in the entire covered temperature range. However, after considering various other possible scattering processes, very good agreement between the experimental and the calculated $\kappa_{a'}(T)$ and $\kappa_{b'}(T)$ curves in the temperature region

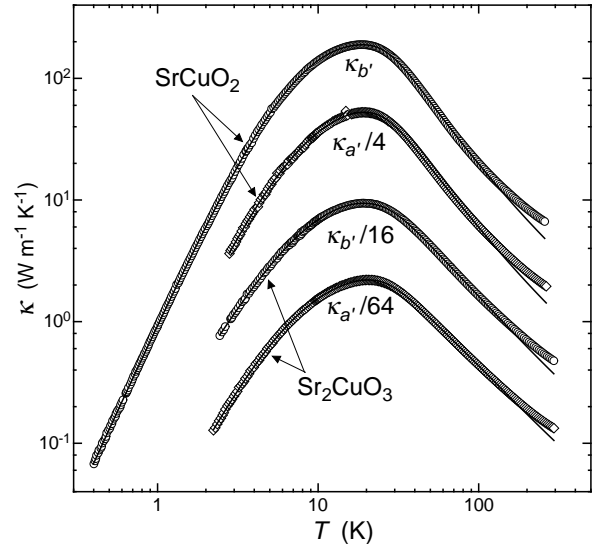


FIG. 3. A comparison of the experimental (open circles and diamonds) and calculated (solid lines) $\kappa(T)$ along the directions perpendicular to the chains. For clarity, the curves for different samples are scaled in order to achieve a reasonable separation between them.

between 0.4 and 100 K was achieved by including two additional terms in Eq. (2). The first one,

$$\tau_d^{-1} = C\omega, \quad (6)$$

where C is a fit parameter, is usually attributed to phonon scattering by strain fields of dislocations.⁴⁰ This term proved to be essential for fitting the temperature dependence of the thermal conductivity at $T < T_{\text{max}}$. The second term is of resonant type⁴¹

$$\tau_{\text{res}}^{-1} = D \frac{\omega^4}{(\omega^2 - \omega_0^2)^2} (1 - cg^2(\omega_0, T)), \quad (7)$$

where ω_0 is the resonance frequency, c is the fractional concentration of scatterers and D is a factor characterizing the strength of the resonant scattering. The function $g(\omega_0, T) \equiv (p_- - p_+)$, describing the difference in population of the upper (p_+) and lower (p_-) states was taken as $g(\omega_0, T) = \tanh(\hbar\omega_0/2k_B T)$, corresponding to a two-level system with singlet upper and lower levels. The parameters D , c , and ω_0 are again fit parameters. A resonant term of this type was initially proposed for phonon scattering by magnetic impurities,⁴¹ but was also successfully used to explain the scattering of acoustic phonons by flat optical phonon modes.⁴²

The fit values of the adjustable parameters L_b , A , B , C , D , ω_0 , c , and b are listed in Table I. The $\kappa(T)$ curves calculated using these values are shown in Fig. 3, together with the experimental data.

For a sample with a rectangular cross-section S_{cs} , a fully diffusive scattering of phonons at the sample boundaries leads to $L_b = 2\sqrt{S_{cs}/\pi}$. The expected values of L_b

compatible with the dimensions of our samples are of the order of 1 mm, i.e., close to the fit values given in Table I. The small values of L_b may possibly be caused by large defects, such as microcracks present in the samples.

The fitting procedure gave values of the parameter A in Eq. (4) equal to 0 or less than 10^{-45} s^3 . With A that small, the influence of point defects on the phonon thermal conductivity is negligible in comparison with other processes of phonon scattering.

For materials with ν atoms in the unit cell, the parameter b in Eq. (5) is expected to be given by $b \sim 2\nu^{1/3}$ (Ref. 43). The fit values of b presented in Table I are in reasonable agreement with this expectation. The parameter B , characterizing the strength of U-processes, depends in a complex manner on elastic and anharmonic constants of a material.

The parameter C , associated with dislocation scattering, is given by⁴⁰

$$C = kn_d \bar{b}^2 \gamma^2, \quad (8)$$

where n_d is the number of dislocations per unit area, \bar{b} is the Burgers vector, γ is the Grüneisen constant, and k is a constant of the order of 10^{-1} . Assuming that $\gamma \sim 2$ and $b \sim 4 \text{ \AA}$, we get $n_d \sim 10^{14} \text{ m}^{-2}$.

The origin of a resonant scattering of phonons in SrCuO_2 and Sr_2CuO_3 is not a priori clear. However, the fact that c defined in Eq. (7) turns out to be close to 1 means that the number of scattering centers is of the order of the number of unit cells in the sample, which severely limits the choice of scattering processes and excludes, for example, dilute magnetic impurities as scatterers. One possible origin of such scattering could be the interaction of acoustic phonons with a flat optical phonon branch, the situation that was promoted in Ref. 42. Another possible source of resonant scattering are excitations of segments of spin chains of finite lengths, created by the inclusion of nonmagnetic defects. In this latter case, the expression for $g(\omega_0, T)$ in Eq. (7) should be changed to describe the degeneracy of the ground and excited states of a chain segment. For chain segments with an even number of spins, which are expected to prevail in $S = 1/2$ AFM Heisenberg chains,⁴⁴ the low-energy resonance corresponds to a singlet-triplet transition and, therefore, $g(\omega_0, T) = (1 - \exp(\hbar\omega_0/k_B T))/(1 + 3 \exp(\hbar\omega_0/k_B T))$. It appears, however, that choosing between $g(\omega_0, T)$ valid for either a singlet-singlet or a singlet-triplet excitation has only a minor effect on the resulting quality of the fit and the values of the parameters in Eq. (7). Therefore, at this point, we cannot distinguish these two possibilities.

As one can see in Fig. 3, the experimental data slightly deviate from the approximation above 100 K. The magnitude of the deviations increases with increasing temperature and, at room temperatures, it is as large as $1.5\text{--}2 \text{ W (m K)}^{-1}$. Experimentally, heat losses by radiation result in measured values of $\kappa(T)$ higher than the intrinsic thermal conductivity. This effect is often observed at

high temperatures for samples with poor thermal conductivity, if no special precautions are taken. Estimates have shown, however, that in our experimental setup the heat losses via radiation are at least an order of magnitude too small to explain the excess conductivity and hence the observed deviation should be attributed to an intrinsic mechanism. Since with increasing temperature the heat is mainly transported by high-frequency phonons for which the Debye model is not a good approximation, the deviations may in principle be attributed to shortcomings of the employed simple model. Another source of high-temperature deviations may be an additional heat transport by optical phonons. We recall that high-temperature deviations of the same magnitude can also be discerned in our $\kappa_{a'}(T)$ data for the spin-ladder system $(\text{Sr,Ca})_{14}\text{Cu}_{24}\text{O}_{41}$.²² The similarity of the high-temperature behavior of $\kappa_{a',b'}(T)$ of spin-chain and spin-ladder materials seems intriguing and may hint to a common origin of the feature such as, as discussed later, diffusive energy transport via the spin system.

C. Phonon thermal conductivity parallel to the chain direction

In contrast to the successful interpretation of the thermal conductivity perpendicular to the chains by considering phonon heat transport alone, we failed completely in obtaining a reasonably good fit of the anomalous T -dependence of $\kappa_{c'}$ at temperatures above T_{max} with a similar approach. In order to emphasize the anomalous feature in $\kappa_{c'}(T)$, we show the anisotropy ratio $\beta = \kappa_{c'}/\kappa_{b'}$ in Fig. 4. For comparison, $\beta = \kappa_{c'}/\kappa_{a'}$ ratios for the spin-ladder system $\text{Sr}_{14-x}\text{Ca}_x\text{Cu}_{24}\text{O}_{41}$ ($x=0, 2$) are included in Fig. 4. At low temperatures the anisotropy is relatively weak and varies little with increasing temperature. A distinct rise of β is observed above 30-40 K.

The obvious similarity of the three systems containing similar Cu-O chains with different interchain interactions suggests a common cause for this anomaly. The anomaly might be due to drastic changes in the phonon heat transport above T_{max} , but we argue below that this is not the case. Indeed, in the vast literature on properties of Sr_2CuO_3 and SrCuO_2 no observation of any phase transition above 6 K has been reported and, therefore, no drastic changes in elastic interatomic interactions at $T > T_{\text{max}}$ is expected. Without such a change affecting the lattice, the chain-like structure of the lattice itself cannot explain the strong temperature-dependent anisotropy of the thermal conductivity above T_{max} . To illustrate this point, we show in the inset of Fig. 4 the anisotropy of the phonon thermal conductivities for Hg_2Cl_2 and Te (data from Refs. 45 and 46, respectively), two chain-type materials with pronounced elastic anisotropies. Hg_2Cl_2 and Te were chosen as examples because in both cases $\kappa(T)$ varies as T^{-1} at high temperatures, i.e., the phonon-phonon scattering dominates

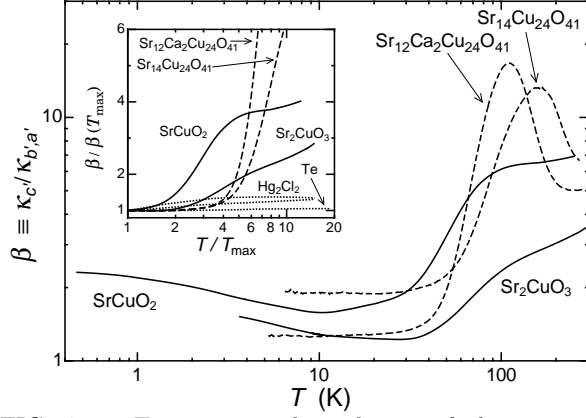


FIG. 4. Temperature dependences of the anisotropy ratios $\kappa_{c'}/\kappa_{b'}$ for SrCuO_2 and Sr_2CuO_3 , and $\kappa_{c'}/\kappa_{a'}$ for $(\text{Sr,Ca})_{14}\text{Cu}_{24}\text{O}_{41}$ (data of Ref. 22). The inset illustrates the relative change of the anisotropies with temperature above T_{max} for the same compounds and also for Hg_2Cl_2 (data of Ref. 45) and Te (data of Ref. 46).

above T_{max} . This demonstrates that even for chain-type materials with strong elastic anisotropies, the anisotropy of the phonon thermal conductivity above T_{max} is only weakly temperature-dependent.

From the point of view of elastic properties, the spin-chain cuprates are rather ordinary, weakly anisotropic materials. For example, the anisotropy of the sound velocities of $\text{Sr}_{14}\text{Cu}_{24}\text{O}_{41}$ is found to be very weak.⁴⁷ Therefore, as we have already argued in Ref. 33, well above T_{max} one may expect not only a weak temperature dependence of β , but also a rather small anisotropy of the phonon-phonon scattering, and therefore $\beta \simeq 1$.

On the other hand, the high-temperature features of $\kappa_{c'}(T)$ do correlate with features in magnetic properties. In Fig. 5 we reproduce the results of Zhai *et al.*⁴⁸ for the dynamic magnetic susceptibilities $\chi_c''(\omega, T)$ of SrCuO_2 , Sr_2CuO_3 , and $\text{Sr}_{14-x}\text{Ca}_x\text{Cu}_{24}\text{O}_{41}$ ($x = 0, 2$) in the c' -direction, measured at $\omega = 10$ GHz. By comparison of Figs. 4 and 5, the correlation between the thermal conductivity and the magnetic susceptibility along the chain direction is obvious⁴⁹ and indicates that the anomalous $\kappa_{c'}(T)$ is of magnetic origin.

Based on the arguments presented above, the increase of $\beta(T)$ for SrCuO_2 and Sr_2CuO_3 with increasing temperature is attributed to an additional, non-phononic channel of heat transport along the chain direction. Most naturally, this excess thermal conductivity is associated with an energy transport via spin excitations of the spin chains. This additional heat transport is large enough to be separated reliably from the phonon contribution.

In order to achieve this separation of the spin-mediated contribution to the thermal conductivity from the experimental data on $\kappa_{c'}$, some assumptions about the phonon background have to be made. As we have argued before,³³ the phonon-phonon scattering is most likely al-

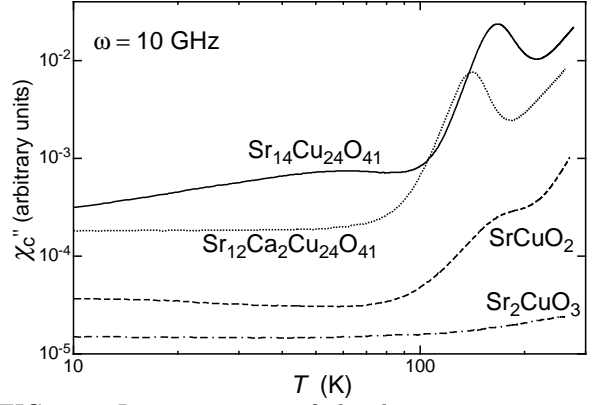


FIG. 5. Imaginary part of the dynamic magnetic susceptibility $\chi_c''(10\text{GHz}, T)$ (reproduced from Ref. 48), for the compounds that are discussed here.

most isotropic. For the evaluation of the relaxation rate via phonon-phonon scattering along the chain direction, one can therefore use the average values of the parameters B and b , obtained by fitting $\kappa(T)$ along the other directions (see Table I). With this assumption, we have fitted the data for $\kappa_{c'}(T)$ at low temperatures ($T \leq 10$ K) where the influence of spin-mediated heat transport, as argued above, is negligible. The fitting procedure was the same as for $\kappa_{a'}$ and $\kappa_{b'}$ but now, only the parameters L , A , C , and D were kept free. For the parameters c (concentration of resonant scatterers) and ω_0 (resonance frequency), again the average values obtained by fitting $\kappa_{a'}(T)$ and $\kappa_{b'}(T)$ were used. The best fits are shown in Fig. 2 as solid lines and the corresponding fit parameters are listed in Table I.

D. Evaluation of the heat transport in the spin system

The spin contribution κ_s to the heat transport along the chain direction was extracted by subtracting the calculated phonon contribution from the experimental data of $\kappa_{c'}(T)$. The resulting $\kappa_s(T)$ dependences are shown in Fig. 6 as open symbols. It is these data that are used for the subsequent analysis of spinon heat transport. However, the way of evaluating κ_s , described above, strongly relies on the assumption of isotropic phonon-phonon scattering. Alternatively, one may consider that the anisotropy of the phonon thermal conductivity does not completely vanish for $T > T_{\text{max}}$, but is similar in magnitude as for the case of chain materials Hg_2I_2 and Te discussed above (see the insert of Fig. 4). The limiting case is then that the anisotropy of the phonon thermal conductivity is constant and equal to that in the region of T_{max} . This situation is illustrated in Fig. 2 where the dashed line represents the phonon thermal conductivity along the c' -axis, averaged along the a' and b' -axes and

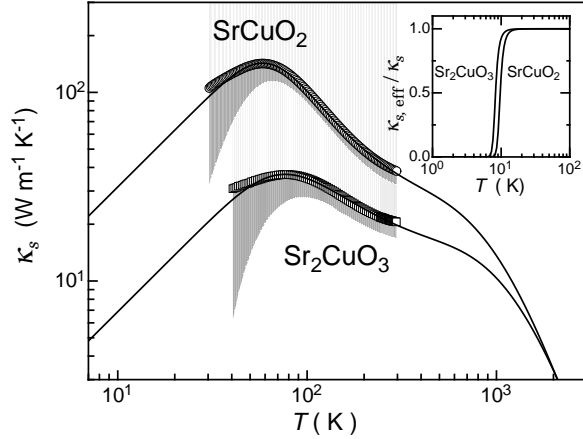


FIG. 6. Spinon thermal conductivity for SrCuO_2 and Sr_2CuO_3 . The solid lines are calculated using Eqs. (14) and (15). The shaded areas demonstrate possible errors caused by the uncertainty of the estimate of the phonon thermal conductivity. The inset shows the ratios between the effective and the intrinsic spinon thermal conductivities, calculated using Eq. (16).

scaled to the value of $\kappa_{c'}(T_{\text{max}})$. The result of subtracting this calculated phonon contribution from the experimental $\kappa_{c'}(T)$ values fixes the lower boundary of possible values of $\kappa_s(T)$ and coincides with the lower edge of the shaded areas in Fig. 6. These areas indicate the possible uncertainty of $\kappa_s(T)$, caused by the ambiguity of our evaluation of the phonon parts of the thermal conductivities. The uncertainty is large at low temperatures, but at higher temperatures it is small enough to allow for a quantitative analysis of the thermal conductivity via spin excitations.

V. ANALYSIS OF THE SPIN CONTRIBUTION

A. Heat transport via diffusion

An important question which can be answered immediately is whether the observed energy transport via spin excitations is diffusive or ballistic. For uniform 1D spin systems the energy transport is expected to be diffusive for spin $S > 1/2$ and ballistic for $S = 1/2$.⁵⁰ However, the diffusive energy transport in $S = 1/2$ chains may be restored by, for example, interchain interactions or intra-chain next-nearest-neighbor interactions.⁵¹ In case of diffusive energy transport, the thermal conductivity is given by $\kappa_s = D_E C_s$, where C_s is the spin specific heat per unit volume and D_E is the energy diffusion constant. In the high-temperature limit, D_E for a quantum spin system is given by $D_E = KJ[S(S+1)]^{1/2}a^2/\hbar$, where a is the distance between neighboring spins and K is a constant which, in different theoretical models, varies between 0.25 and 3.⁵² In the low-temperature region, D_E is expected

to be nearly independent of temperature.⁵³ Using, for the specific heat, the low-temperature ($T \ll J/k_B$) result of a Bethe ansatz solution⁵⁴ for a uniform chain of N spins $S = 1/2$

$$C_s = \frac{2Nk_B^2}{3J}T, \quad (9)$$

the thermal conductivity in the diffusive regime is

$$\kappa_s \sim n_s \frac{a^2 k_B^2}{\hbar} T. \quad (10)$$

Here, n_s is the number of spins per unit volume. Eq. (10) predicts rather small values for κ_s (of the order of 1 W (m K)^{-1} at 300 K) decreasing linearly with decreasing temperatures. The observed $\kappa_s(T)$ along the c' -axis is much higher than predicted by Eq. (10) and, at least at $T > 80 \text{ K}$, it increases with decreasing temperature. This is a clear sign of non-diffusive energy transport via spin excitations along the chains, in agreement with theoretical predictions. It is worth noting that also the spin diffusion constant D_S has experimentally been found to be strongly enhanced in Sr_2CuO_3 .⁵⁵ This observation was considered as indicating the ballistic nature of spin transport.

In contrast to the c' -direction, the high-temperature excess thermal conductivity along the a' and b' directions, discussed in section IV B, is in fair agreement with Eq. (10) both in absolute values and with respect to its temperature dependence. We therefore argue that the possible energy transport perpendicular to the Cu-O chains via the spin system is small and diffusive. On the contrary, the energy transport via spins along the chains is substantial and relies on the ballistic propagation of spin excitations, interacting with lattice imperfections and other quasiparticles.

B. Spinon heat transport along the chain direction

As mentioned in the introduction, the elementary excitations of a uniform Heisenberg 1D AFM $S = 1/2$ system carry a spin $S = 1/2$.⁷ Therefore the low-temperature thermodynamic behavior of such an ensemble can be accounted for by using the usual Fermi-Dirac distribution $f = (\exp(\varepsilon/k_B T) + 1)^{-1}$ with zero chemical potential,⁸ where ε is the spinon energy. The dispersion relation for spinons is given by⁷

$$\varepsilon(k) = \frac{J\pi}{2} |\sin ka|. \quad (11)$$

For spinons, the possible values of the wave vector k are restricted to one half of the Brillouin zone. The low-temperature specific heat, calculated using the general equation

$$C_s = \frac{2Na}{\pi} \int_0^{\pi/2a} \frac{\partial f}{\partial T} \varepsilon dk, \quad (12)$$

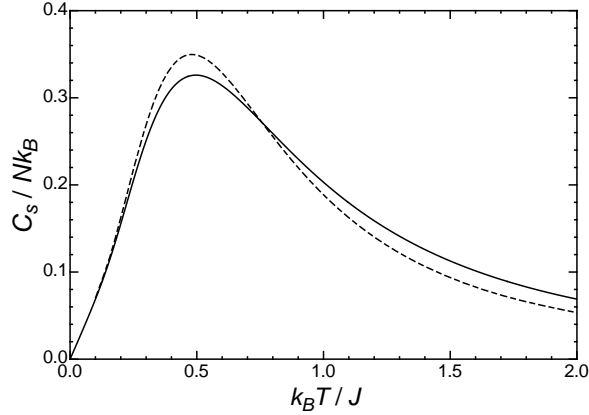


FIG. 7. The specific heat of the $S=1/2$ AFM Heisenberg chain, calculated using Eq. (12) (solid line) and the Bethe ansatz solution (dashed line, data from Ref. 57).

agrees with the low-temperature result of Eq. (9). As illustrated in Fig. 7, the high-temperature specific heat calculated with Eq. (12) qualitatively reproduces the main high-temperature features of the results of the Bethe ansatz solution.^{56,57} The disagreement between the two models is not important for our analysis since our results have been obtained in the low temperature region $k_B T / J < 0.15$.

Applying the Boltzmann-type approximation, the thermal conductivity of a spinon system is

$$\kappa_s = \frac{2n_s a}{\pi} \int_0^{\pi/2a} \frac{\partial f}{\partial T} \varepsilon v_s l_s dk, \quad (13)$$

where $v_s = \hbar^{-1} \partial \varepsilon / \partial k$ is the group velocity and l_s is the mean free path of a spinon. Cast in another but equivalent form,

$$\kappa_s = \frac{2n_s k_B^2 a}{\pi \hbar} T \int_0^{J\pi/2k_B T} \frac{x^2 e^x}{(e^x + 1)^2} l_s(\varepsilon, T) dx, \quad (14)$$

where $x = \varepsilon / k_B T$. If several independent scattering mechanisms have to be considered, the spinon mean free path can be represented as $l_s^{-1}(\varepsilon, T) = \sum l_{s,i}^{-1}(\varepsilon, T)$, where each $l_{s,i}(\varepsilon, T)$ term corresponds to an independent scattering channel. This is analogous to the case of phonons, considered in Eq. (2).

The most straightforward way to analyze our $\kappa_s(T)$ data would be analogous to that employed for the phonon conductivity, i.e., by choosing a set of $l_{s,i}(\varepsilon, T)$ terms in the equation for the mean free path of spinons and fitting the data of $\kappa_s(T)$ to Eq. (14). However, the energy and temperature dependences for most of the plausible scattering mechanisms have not yet been worked out. That is why we treated the $\kappa_s(T)$ data by inserting the spinon

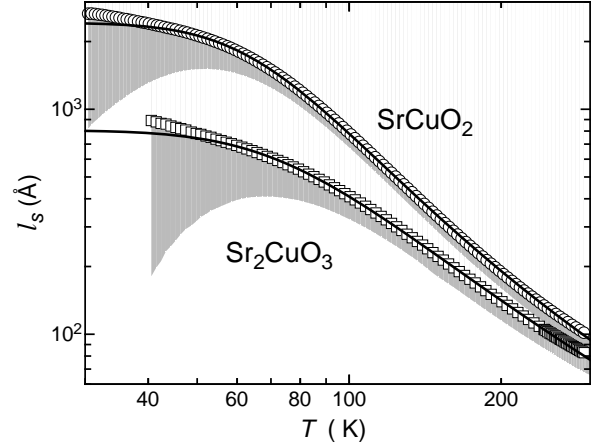


FIG. 8. The temperature dependences of the spinon mean free paths for Sr_2CuO_3 and SrCuO_2 , calculated using Eq. (14). The solid lines are fits using Eq. (15). The shaded areas have the same meaning as in Fig. 6.

mean free path $l_s(T)$, averaged over all ε , at a given temperature. In that case, $l_s(T)$ may be taken out of the integral in Eqs. (13) and (14) and thus may be calculated from the $\kappa_s(T)$ data, using the known values of J for the materials investigated here. For these calculations, $J/k_B = 2100$ K (Ref. 28) and 2620 K (Ref. 33) were used for SrCuO_2 and Sr_2CuO_3 , respectively. The resulting values of $l_s(T)$ for SrCuO_2 and Sr_2CuO_3 are shown in Fig. 8.

Here again, the shaded areas reveal the possible range of l_s values caused by the uncertainties in evaluating the phonon thermal conductivities. In Ref. 33, it was noted that $l_s(T)$ for Sr_2CuO_3 may be approximated by

$$l_s^{-1} = l_{sp}^{-1} + l_{sd}^{-1} = A_{sp} T \exp(-T^*/T) + L_{sd}^{-1}, \quad (15)$$

where the two terms were attributed to spinon scattering by phonons and defects, respectively. Here, the parameter A_{sp} characterizes the strength of spin-lattice interaction, T^* is related to the minimum energy needed to produce a single spinon-phonon Umklapp-process, and L_{sd} is the mean distance between magnetic defects effectively scattering spin excitations in a spin chain. It may be seen that with Eq. (15) and the appropriate parameters, $l_s(T)$ may be well approximated not only for Sr_2CuO_3 but also for SrCuO_2 . The values of $A_{sp} = 7.1 \times 10^5 \text{ m}^{-1}\text{K}^{-1}$, $T^* = 177 \text{ K}$, $L_{sd} = 8.1 \times 10^{-8} \text{ m}$ for Sr_2CuO_3 , and $A_{sp} = 6.7 \times 10^5 \text{ m}^{-1}\text{K}^{-1}$, $T^* = 204 \text{ K}$, $L_{sd} = 2.42 \times 10^{-7} \text{ m}$ for SrCuO_2 , were obtained by fitting the data of $l_s(T)$ with Eq. (15). The fits are shown as solid lines in Fig. 8. The parameter values for Sr_2CuO_3 are slightly different from those presented in Ref. 33, because of a somewhat different way of evaluating the phonon thermal conductivity. The agreement between the experimental data and the fit is very good above approximately 50 K, but at lower temperatures the uncertainty in extracting $l_s(T)$ becomes far too large to draw

any reliable conclusion concerning its temperature dependence and the involved scattering mechanisms.

The fit values of the parameters A_{sp} and T^* which are related to the spin-lattice interaction are similar in magnitude for the two compounds, in spite of the different chain arrangements. The values of T^* scale with the Debye temperatures, supporting the idea that the term l_{sp}^{-1} in Eq. (15) is indeed related to the spin-lattice interaction. It appears that the main difference between the two materials is in the defect scattering, which is three times more efficient for Sr_2CuO_3 than for SrCuO_2 . The low-temperature values of l_s for Sr_2CuO_3 have been found³³ to be in fair agreement with the mean distance between neighboring bond-defects causing local changes in the magnetic coupling between Cu spins, as extracted from NMR data.⁵⁸ Unfortunately, similar NMR results revealing the distance between bond-defects are absent for SrCuO_2 . Our data suggest an about three times smaller concentration of these defects in SrCuO_2 than in Sr_2CuO_3 .

C. Influence of spinon-phonon scattering

For the two investigated materials, the evaluation of the spinon part of the thermal conductivity has been achieved only in a limited temperature region, characterized by $0.015 \leq T/J \leq 0.15$. Two mechanisms of spinon scattering seem to be effective, namely the temperature-dependent spinon-phonon interaction and the temperature-independent scattering of spinons by defects. The significance of other scattering mechanisms, if any, is negligible. For example, normal processes of spinon-spinon scattering cannot change the total momentum of the spinon system and, therefore, should not contribute to the thermal resistance. The spinon-spinon Umklapp-processes are expected to play a serious role only at temperatures $T \sim J/k_B$.

Supposing that the validity of Eq. (15) extends beyond the region $0.015 \leq T/J \leq 0.15$, we may estimate the expected spinon thermal conductivity at lower and higher temperatures using Eq. (14). The result is shown as solid lines in Fig. 6. Since $l_s(T)$ is constant and equal to L_{sd} at very low temperatures, $\kappa_s(T)$ is expected to vary linearly with T as $\kappa_s = n_s a k_B^2 \pi L_{sd} T / 3\hbar$. The phonon thermal conductivity varies as T^3 at low temperatures and hence the spinon contribution should progressively dominate with decreasing temperature. This expectation is obviously not met by our low-temperature results. First of all, no linear contribution to the total measured thermal conductivity has been identified and, second, no distinct feature in $\kappa(T)$ is observed at the Néel temperature T_N , indicating a negligible spinon contribution κ_s . This suggests that at some temperature below 30 K the spinon contribution deviates from the predicted behavior shown in Fig. 6 and by 6 K, spinons are excluded from heat transport. At this point, a discussion of the spin-lattice

interaction is in order.

Although the spin-lattice interaction reduces both the phonon- and the spin-related thermal conductivities because of scattering processes involving both types of quasiparticles, some degree of it is needed for the spin-related heat conduction to be observable in a thermal conductivity experiment.⁵⁹ The energy provided by a heater generates only phonons, and the spin-phonon interaction is needed for an energy transfer from the lattice to the spin system. The effective spinon thermal conductivity $\kappa_{s,\text{eff}}$ which is accessible in a coupled spin-lattice system, is⁵⁹

$$\kappa_{s,\text{eff}} = (\kappa_s + \kappa_{ph}) \left(1 + \frac{\kappa_s}{\kappa_{ph}} \frac{\tanh(AL_{\text{sample}}/2)}{AL_{\text{sample}}/2} \right)^{-1} - \kappa_{ph}, \quad (16)$$

where L_{sample} is the sample length,

$$A = \left(\tau_{sp}^{-1} \frac{\kappa_s^{-1} + \kappa_{ph}^{-1}}{C_{ph}^{-1} + C_s^{-1}} \right)^{1/2}, \quad (17)$$

and τ_{sp} is the spin-lattice relaxation time. For very short spin-lattice relaxation times ($\tau_{sp}^{-1} \rightarrow \infty$), $\kappa_{s,\text{eff}} = \kappa_s$. In the opposite case of a very weak spin-lattice interaction ($\tau_{sp}^{-1} \rightarrow 0$), however, $\kappa_{s,\text{eff}} = 0$ and the thermal transport by spinons cannot be observed in an experiment, regardless of how large the intrinsic κ_s of the sample is.

If the first term in Eq. (15) is indeed dictated by the spin-lattice interaction, it is possible to establish the temperature region in which the observed $\kappa_{s,\text{eff}}$ equals the intrinsic κ_s . For this purpose, the ratio $\kappa_{s,\text{eff}}/\kappa_s$ was calculated by assuming $\tau_{sp} = l_{sp}/v_s$ (see Eq. (15)) and $v_s = Ja\pi/2\hbar$, valid for low-energy spinons which dominate at $T \ll J/k_B$. The result is shown in the inset of Fig. 6. Although the extrapolation of Eq. (15) to lower temperatures may not exactly be correct, it is nevertheless clear (see the inset of Fig. 6) that at very low temperatures the spin-lattice interaction turns out to be too weak for the spinon thermal conductivity to be observed.

From our discussion it is obvious that the interaction between the spin and the phonon system should show up both in spinon and phonon heat transport. However, other mechanisms of phonon scattering, mainly the phonon-phonon interaction, may be stronger and mask the scattering of phonons by spin excitations. This may be the reason why a term corresponding to the phonon-spinon scattering does not have to be included in Eq. (2) for a reasonable description of $\kappa_{ph}(T)$. On the other hand, a phonon-spinon relaxation rate $\bar{\tau}_{ps}(T)$, averaged over the entire phonon spectrum at a given temperature, may roughly be approximated by

$$\bar{\tau}_{ps}^{-1} \sim \frac{N_s}{N_{ph}} \tau_{sp}^{-1}, \quad (18)$$

where at a fixed temperature T , $N_{ph}(T)$ and $N_s(T)$ are the average numbers of phonons and spinons per unit

volume, respectively. At high temperatures, where spin-phonon interaction is important, Eq. (18) for the phonon-spinon scattering rate gives $\bar{\tau}_{ps}^{-1} \propto T \exp(-T^*/T)$, i.e., the same temperature dependence as is characteristic for the phonon-phonon interaction. That is why, even if the influence of phonon scattering by spin excitations is not negligible, it is difficult to separate it from the phonon-phonon interaction.

In the present discussion, we do not consider the possibility of a mutual drag between spin and lattice excitations, which may be considerable under certain conditions, as described in Ref. 60.

VI. SUMMARY

In this paper the thermal conductivities of the spin-chain compounds SrCuO_2 and Sr_2CuO_3 were studied. Although the crystal structures of the two compounds are different in the sense that the former contains linear and the latter zig-zag Cu-O chains, the thermal conductivity of both materials is remarkably similar. In particular, the heat transport in the directions perpendicular to the chains is dominated by phonons, but along the chain direction and at high temperatures there is a substantial excess contribution related to the transport of energy by spinons.

The phonon thermal conductivity is analyzed employing a Debye-type approximation. The main sources of phonon scattering are phonons at high temperatures and lattice defects, presumably dislocations, at low temperatures. The spin-phonon interaction is not seen in the phonon heat transport, most likely because it is masked by other scattering processes.

An eventual energy transport via the spin system in the directions perpendicular to the spin chains is found to be small and, if any at all, of diffusive character. On the contrary, the spin-mediated energy transport along the chain direction is large and propagating ballistically. The contribution of spin excitations (spinons) is reliably singled out along the chain direction at high temperatures where it exceeds the phonon contribution quite substantially. Our analysis based on a fermion model suggests that the expected infinite spinon thermal conductivity is limited by the influence of defects and phonons.

ACKNOWLEDGMENTS

This work was financially supported in part by the Schweizerische Nationalfonds zur Förderung der Wissenschaftlichen Forschung.

- ¹ C. Giardiná, R. Livi, A. Politi, and M. Vassalli, *Phys. Rev. Lett.* **84**, 2144 (2000).
- ² O. V. Gendelman and A. V. Savin, *Phys. Rev. Lett.* **84**, 2381 (2000).
- ³ B. Hu, B. Li, and H. Zhao, *Phys. Rev. E* **61**, 3828 (2000).
- ⁴ H. Castella, X. Zotos, and P. Prelovšek, *Phys. Rev. Lett.* **74**, 972 (1995).
- ⁵ K. Saito, S. Takesue, and S. Miyashita, *Phys. Rev. E* **54**, 2404 (1996).
- ⁶ X. Zotos, F. Naef, and P. Prelovšek, *Phys. Rev. B* **55**, 11029 (1997).
- ⁷ L. D. Faddeev and L. A. Takhtajan, *Phys. Lett.* **85A**, 375 (1981).
- ⁸ W. McRae and O. P. Sushkov, *Phys. Rev. B* **58**, 62 (1998).
- ⁹ B. A. Bernevig, D. Giuliano, and R. B. Laughlin, *cond-mat/0011270*.
- ¹⁰ M. Schöbinger and R. J. Jelitto, *Z. Phys. B* **43**, 199 (1981).
- ¹¹ J. A. H. M. Buijs and W. J. M. de Jonge, *J. Phys. C* **15**, 6631 (1982).
- ¹² G. M. Wysin and P. Kumar, *Phys. Rev. B* **36**, 7063 (1987).
- ¹³ H. A. M. de Gronckel, W. J. M. de Jonge, K. Kopinga, and L. F. Lemmens, *Phys. Rev. B* **44**, 4654 (1991).
- ¹⁴ S. N. Evangelou and S. J. Xiong, *J. Phys.: Condens. Matter* **8**, 1051 (1996).
- ¹⁵ V. G. Bar'yakhtar and B. A. Ivanov, *Sov. Sci. Rev. A. Phys.* **16**, 1 (1992).
- ¹⁶ J. Rácz, *J. Stat. Phys.* **101**, 273 (2000).
- ¹⁷ X. Zotos, F. Naef, and P. Prelovšek, *cond-mat/9906441*.
- ¹⁸ O. P. Sushkov, *Phys. Rev. B* **60**, 14517 (1999).
- ¹⁹ H. Miike and K. Hirakawa, *J. Phys. Soc. Jpn.* **38**, 1279 (1975).
- ²⁰ J. Takeya, I. Tsukada, Y. Ando, T. Masuda, and K. Uchinokura, *Phys. Rev. B* **62**, 9260 (2000).
- ²¹ M. Köppen, M. Lang, R. Helfrich, F. Steglich, P. Thalmeier, B. Schmidt, B. Wand, D. Pankert, H. Benner, H. Aoki, and A. Ochiai, *Phys. Rev. Lett.* **82**, 4548 (1999).
- ²² A. V. Sologubenko, K. Giannò, H. R. Ott, U. Ammerahl, and A. Revcolevschi, *Phys. Rev. Lett.* **84**, 2714 (2000).
- ²³ K. Kudo, S. Ishikawa, T. Noji, T. Adachi, Y. Koike, K. Maki, S. Tsuji, and K. Kumagai, *J. Phys. Soc. Jpn* **70**, 437 (2001).
- ²⁴ C. L. Teske and H. Müller-Buschbaum, *Z. Anorg. Allg. Chem.* **371**, 325 (1969).
- ²⁵ C. L. Teske and H. Müller-Buschbaum, *Z. Anorg. Allg. Chem.* **379**, 234 (1970).
- ²⁶ T. Ami, M. K. Crawford, R. L. Harlow, Z. R. Wang, D. C. Johnston, Q. Huang, and R. W. Erwin, *Phys. Rev. B* **51**, 5994 (1995).
- ²⁷ H. Suzuura, H. Yasuhara, A. Furusaki, N. Nagaosa, and Y. Tokura, *Phys. Rev. Lett.* **76**, 2579 (1996).
- ²⁸ N. Motoyama, H. Eisaki, and S. Uchida, *Phys. Rev. Lett.* **76**, 3212 (1996).
- ²⁹ D. C. Johnston, *Acta Phys. Pol. A* **91**, 181 (1997).
- ³⁰ R. S. Eccleston, M. Uehara, A. J. H. Eisaki, N. Motoyama, and S. Uchida, *Phys. Rev. Lett.* **81**, 1702 (1998).
- ³¹ T. M. Rice, S. Gopalan, and M. Sigrist, *Europhys. Lett.* **23**, 445 (1993).
- ³² S. R. White and I. Affleck, *Phys. Rev. B* **54**, 9862 (1996).
- ³³ A. V. Sologubenko, E. Felder, K. Giannò, H. R. Ott, A. Vitekine, and A. Revcolevschi, *Phys. Rev. B* **62**, 6108 (2000).

- ³⁴ A. Revcolevschi, A. Vietkine, and H. Moudden, *Physica C* **282-287**, 493 (1997).
- ³⁵ A. Keren, L. P. Le, G. M. Luke, B. J. Sternlieb, W. D. Wu, Y. J. Uemura, S. Tajima, and S. Uchida, *Phys. Rev. B* **48**, 12926 (1993).
- ³⁶ K. M. Kojima, Y. Fudamoto, M. Larkin, G. M. Luke, J. Merrin, B. Nachumi, Y. J. Uemura, N. Motoyama, H. Eisaki, S. Uchida, K. Yamada, Y. Endoh, S. Hosoya, B. J. Sternlieb, and G. Shirane, *Phys. Rev. Lett.* **78**, 1787 (1997).
- ³⁷ M. Matsuda, K. Katsumata, K. M. Kojima, M. Larkin, G. M. Luke, J. Merrin, B. Nachumi, Y. J. Uemura, H. Eisaki, N. Motoyama, S. Uchida, and G. Shirane, *Phys. Rev. B* **55**, 11953 (1997).
- ³⁸ I. A. Zaliznyak, C. Broholm, M. Kibune, M. Nohara, and H. Takagi, *Phys. Rev. Lett.* **83**, 5370 (1999).
- ³⁹ M. Matsuda, private communication.
- ⁴⁰ P. G. Klemens, in *Solid State Physics*, edited by F. Seitz and D. Turnbull (Academic, New York, 1958), Vol. 7, p. 1.
- ⁴¹ F. W. Sheard and G. A. Toombs, *Solid State Commun.* **12**, 713 (1973).
- ⁴² M. N. Wybourne, B. J. Kiff, D. N. Batchelder, D. Greig, and M. Sahota, *J. Phys. C* **18**, 309 (1985).
- ⁴³ G. A. Slack, in *Solid State Physics*, edited by H. Ehrenreich, F. Seitz, and D. Turnbull (Academic, New York, 1979), Vol. 34, p. 1.
- ⁴⁴ M. Nishino, H. Onishi, P. Roos, K. Yamaguchi, and S. Miyashita, *Phys. Rev. B* **61**, 4033 (2000).
- ⁴⁵ M. B. Koss, K. A. McCarthy, and H. H. Sample, *Phys. Rev. B* **42**, 5822 (1990).
- ⁴⁶ A. R. Adams, F. Baumann, and J. Stuke, *Phys. Status Solidi* **23**, K99 (1967).
- ⁴⁷ D. König, U. Löw, S. Schmidt, H. Schwenk, M. Sieling, W. Palme, B. Wolf, G. Bruls, B. Lüthi, M. Matsuda, and K. Katsumata, *Physica B* **237-238**, 117 (1997).
- ⁴⁸ Z. Zhai, P. V. Patanjali, N. Hakim, J. B. Sokoloff, S. Sridhar, U. Ammerahl, A. Vietkine, and A. Revcolevschi, *cond-mat/9903198*.
- ⁴⁹ The fact that the absolute temperatures of the anomalies are not exactly the same for $\beta(T)$ and $\chi_c''(\omega, T)$ should not be overrated because the temperatures of the $\chi_c''(\omega, T)$ peaks are frequency-dependent and shift to lower temperatures for lower ω (Ref. 48).
- ⁵⁰ D. L. Huber and J. S. Semura, *Phys. Rev.* **182**, 602 (1969).
- ⁵¹ D. A. Krueger, *Phys. Rev. B* **3**, 2348 (1971).
- ⁵² D. L. Huber, J. S. Semura, and C. G. Windsor, *Phys. Rev.* **186**, 534 (1969).
- ⁵³ D. L. Huber, *Prog. Theor. Phys.* **39**, 1170 (1968).
- ⁵⁴ M. Takahashi, *Prog. Theor. Phys.* **50**, 1519 (1973).
- ⁵⁵ M. Takigawa, N. Motoyama, H. Eisaki, and S. Uchida, *Phys. Rev. Lett.* **76**, 4612 (1996).
- ⁵⁶ H. W. J. Blöte, *Physica* **78**, 302 (1974).
- ⁵⁷ A. Klümper and D. C. Johnston, *Phys. Rev. Lett.* **84**, 4701 (2000).
- ⁵⁸ J. P. Boucher and M. Takigawa, *Phys. Rev. B* **62**, 367 (2000).
- ⁵⁹ D. J. Sanders and D. Walton, *Phys. Rev. B* **15**, 1489 (1977).
- ⁶⁰ L. E. Gurevich and G. A. Roman, *Fiz. Tverd. Tela* (Leningrad) **8**, 2628 (1966) [*Sov. Phys. - Solid State* **8**, 2102 (1967)].

TABLE I. Parameters of the fitting of $\kappa(T)$ data to Eq. (1).

Parameter	SrCuO ₂ <i>a'</i> -axis	SrCuO ₂ <i>b'</i> -axis	Sr ₂ CuO ₃ <i>a'</i> -axis	Sr ₂ CuO ₃ <i>b'</i> -axis	SrCuO ₂ <i>c'</i> -axis	Sr ₂ CuO ₃ <i>c'</i> -axis
L (10^{-3} m)	0.32 ± 0.1	0.25 ± 0.02	0.97 ± 0.5	8 ± 6	0.63 ± 0.04	2.5 ± 2
A (10^{-42} s ³)	$< 10^{-45}$	$< 10^{-45}$	$< 10^{-45}$	$< 10^{-45}$	$< 10^{-45}$	$< 10^{-45}$
B (10^{-18} s K ⁻¹)	11.1 ± 0.5	13.5 ± 0.5	7.6 ± 0.5	9.0 ± 0.5	12.3	8.30
b	2.7 ± 0.2	2.8 ± 0.1	3.5 ± 0.3	3.3 ± 0.2	2.75	3.4
C (10^{-6})	7.2 ± 1	5.8 ± 0.3	9.4 ± 1	10.6 ± 0.7	3.9 ± 0.2	5.5 ± 0.2
D (10^9 s ⁻¹)	4.6 ± 2	2.7 ± 1	5.6 ± 3	6.5 ± 2.5	3.5 ± 1	7.7 ± 0.2
ω_0 (10^{12} s ⁻¹)	10.0 ± 1	8.3 ± 1.5	10.2 ± 1	9.6 ± 1	9.2	9.9
c	0.86 ± 0.03	0.90 ± 0.01	0.76 ± 0.03	0.87 ± 0.03	0.88	0.815
Temperature region	$T < 100$ K	$T < 100$ K	$T < 100$ K	$T < 100$ K	$T < 12$ K	$T < 13$ K